Front. Optoelectron. 2015, 8(4): 379–393
DOI 10.1007/s12200-014-0423-5

REVIEW ARTICLE

Optical approaches in study of nanocatalysis with single-molecule and single-particle resolution

Kun LI, Weiwei QIN, Yan XU, Tianhuan PENG, Di LI (✉)

Division of Physical Biology & Bioimaging Center, Shanghai Synchrotron Radiation Facility, Shanghai Institute of Applied Physics, Chinese Academy of Sciences, Shanghai 201800, China

Abstract Studying the activity of individual nanocatalysts, especially with high spatiotemporal resolution of single-molecule and single-turnover scale, is essential for the understanding of catalytic mechanism and the designing of effective catalysts. Several approaches have been developed to monitor the catalytic reaction on single catalysts. In this review, we summarized the updated progresses of several new spectroscopic and microscopic approaches, including single-molecule fluorescence microscopy, surface-enhanced Raman spectroscopy, surface plasmon resonance microscopy and X-ray microscopy, for the study of single-molecule and single-particle catalysis.

Keywords nanocatalysis, single-molecule fluorescence, surface-enhanced Raman, localized surface plasmon resonance, X-ray

1 Introduction

Heterogeneous catalysts made of various materials play a crucial role in modern chemistry, ranging from fine chemical synthesis, energy conversions to pollutant removals [1–3]. Traditional studies of catalysts are focused on ensemble-averaged measurements, assuming that heterogeneous catalysts and catalytic events are spatial and temporal homogeneous. However, due to the complexity of heterogeneous reaction and heterogeneities of individual catalyst particles in both size and morphology, detailed chemical information obtained on heterogeneous catalysts is scarce, leading to a lack of insight understanding of chemical processes. Even on single nanoparticle, active sites come from different types of surface sites such as corner, edge and facet sites, with intrinsically heterogeneities of their nature, distribution and accessibility [4]. In addition to the above mentioned spatial differences, each single catalytic turnover is always transitory due to the morphology changes and surface structural dynamics of catalysts. Therefore, studies of catalytic reactions in real time, and at the single-molecule and single-particle level are needed to address these key challenges [5,6].

Metal nanoparticles (NPs) are important heterogeneous catalysts for many chemical transformations due to their nanometer size-induced high surface-to-volume ration and high chemical potentials [7–9]. The advance in chemical synthesis has allowed the preparation of catalytic nanoparticles, or nanocatalysts, with impressive control of size, shape and composition [10–12]. Even though, studies of nanocatalysts still suffer from lack of sufficient spatiotemporal resolution to gain further direct insights into catalytic mechanism.

Recently, we have witnessed the introduction of some novel spatiotemporal spectroscopy for the characterization of nanocatalysts with unattainable resolution and sensitivity. Figure 1 illustrates the complexity and size of the individual catalyst particle under study (left side), and distinct analysis methods with different spatial resolution and chemical information content (right side). Depending on the chemical information needed and the spatial resolution at which the catalyst material functions, a suitable characterization method [4] can be selected for the evaluation of heterogeneities in space and time for both model catalyst particles (for example large zeolite crystals and metal particles) and real, industrially used catalyst particles (for example catalyst bodies, small zeolite crystals and supported metal nanoparticles).

In this review, we focus on optical approaches in the study of nanocatalysis with single-molecule and single-particle resolution. These spectroscopic and microscopic methods rely on the sensitive detection of optical signals

Received February 27, 2014; accepted March 4, 2014

E-mail: lidi@sinap.ac.cn

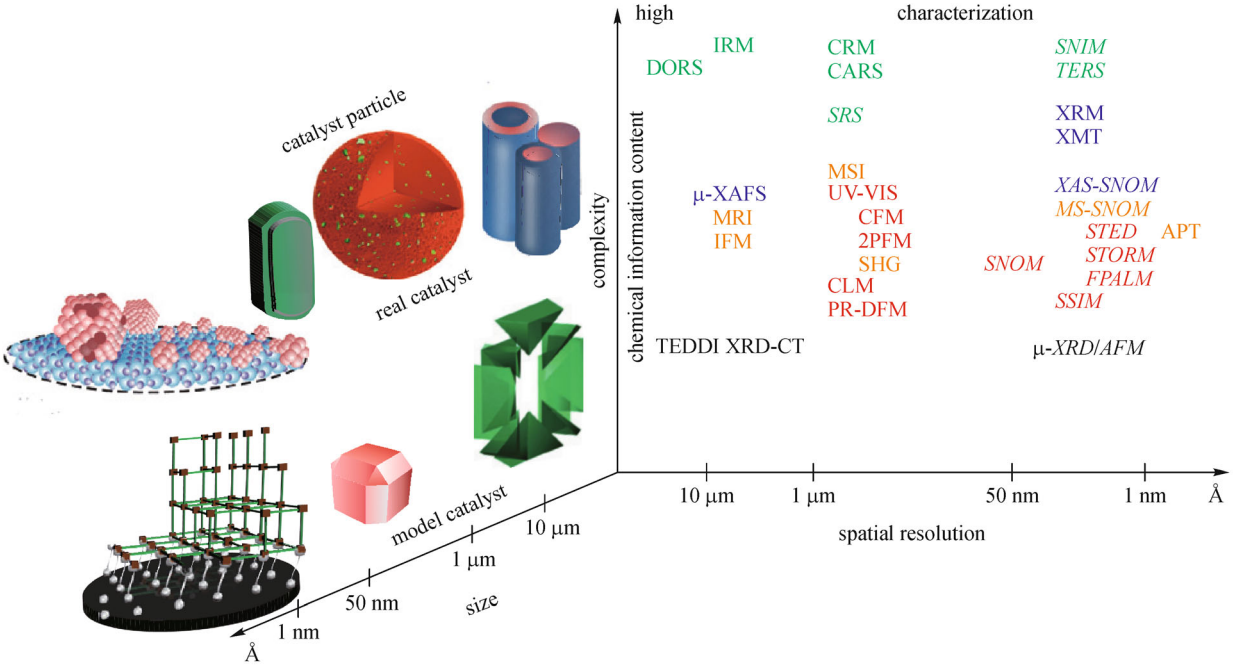

Fig. 1 Chemical imaging methods that are available or will become available in the future (in italics), for the investigation of catalysts at the single-particle level. The abbreviations of the included characterization techniques are as follows. Vibrational spectroscopy methods (green): DORS, diagonally offset Raman spectroscopy; IRM, infrared microscopy; CRM, confocal Raman microscopy, CARS, coherent anti-Stokes Raman spectroscopy; SRS, stimulated Raman scattering microscopy; SNIM, scanning near-field infrared microscopy; TERS, tip-enhanced Raman spectroscopy. X-ray spectroscopy methods (blue): μ-XAFS, microbeam X-ray absorption fine structure spectroscopy; XRM, X-ray microscopy; XMT, X-ray microtomography; XAS-SNOM, X-ray absorption spectroscopy/scanning near-field optical microscopy. Electronic spectroscopy methods (red): UV-VIS, ultraviolet–visible microscopy; CFM, confocal fluorescence microscopy; 2PFM, two-photon fluorescence microscopy; CLM, chemiluminescence microscopy; PR-DFM, plasmon resonance dark field microscopy; STED, stimulated emission depletion microscopy; STORM, stochastic optical reconstruction microscopy; FPALM, fluorescence photo-activated localization microscopy; SSIM, saturated structured illumination microscopy. X-ray diffraction methods (black): TEDDI, tomographic energy-dispersive diffraction imaging; XRD-CT, X-ray diffraction-computed tomography; μ-XRD/AFM, microbeam X-ray diffraction/atomic force microscopy. Miscellaneous (orange): MRI, magnetic resonance imaging; IFM, interference microscopy; MSI, mass spectrometry imaging; SHG, second-harmonic generation microscopy; MS-SNOM, mass spectrometry/scanning near-field optical microscopy. Adapted with permission from Ref. [4], copyright 2012 Nature Publishing Group

arising from reactants, products, nanocatalysts, or changes of the surroundings evoked by these reactions. Other methods, for instance, electrochemical measurements with ultramicroelectrode [13] and scanning electrochemical microscopy [14], which are capable of measuring catalysis on single particles, but failed to achieve single-reaction resolution for each reaction only resulting in the transfer of one or few electrons, are not covered.

2 Optical responses from reactants and products

In catalysis, reactants in gas or liquid phase are often converted to desired product molecules on the surface of catalytically active nanoparticles. Thus, a direct means to monitoring catalysis on a single nanoparticle is to detect the optical response changes of reactants or products. This requires ultrasensitive optical resolution because in each catalytic turnover, only one or a few molecules may be consumed or generated on a single nanoparticle.

2.1 Single-molecule fluorescence microscopy

This approach builds on the pioneering work in single-enzyme catalysis [15–20]. Roeffaers et al. [21] in 2006, first employed the knowledge obtained from single molecule enzymology and studied the spatial distribution of catalytic activity on a layered double hydroxide crystal. After that, several catalysis research works in studying micro- and nano-scale solid catalysts based on this method were continuing to emerge [22,23]. In this strategy, a fluorogenic substrate is catalytically converted into a strongly fluorescent product, which is then optically detected by total-internal-reflection fluorescence microscopy (TIRFM) [5,24,25].

TIRFM employs the unique properties of an induced evanescent wave to selectively illuminate and excite

fluorophores in a restricted specimen region immediately adjacent to a glass-water (or glass-buffer) interface. The basic concept of TIRFM is simple, requiring only an excitation light beam traveling at a high incident angle through the solid glass coverslip or plastic tissue culture container, where the cells adhere. Refractive index differences between the glass and water phases regulate how light is refracted or reflected at the interface as a function of incident angle. At a specific critical angle, the beam of light is totally reflected from the glass/water interface, rather than passing through and refracting in accordance with Snell's Law. The reflection generates a very thin electromagnetic field (usually less than 200 nm) in the aqueous medium, which has an identical frequency to that of the incident light, which enables to detect a single fluorescence molecule [26].

Real-time single-molecule kinetics of single nanoparticles Chen and coworkers [23,27–30] detected the catalytic activity of individual 6 nm gold (Au) nanoparticles with single turnover precision. The single-molecule turnover of non-fluorescent resazurin to its fluorescent product resorufin by the addition of NH_2OH was monitored as a reporter system (Fig. 2(a)). A continuous flow was applied to accelerate the release of product molecules from the nanoparticles after a short period of stay, leading to a sudden disappearance of the fluorescence emission and an unoccupied nanoparticle for the next chemical reactions. Individual catalytic reactions on a single Au nanoparticle are reported by the fluorescence bursts at a localized spot on the image, corresponding with fluorescence intensity *vs.* time trajectory (Fig. 2(d)). Based on the stochastic analysis of the on- and off-times of fluorescence bursts measured at different substrate concentrations, both the kinetics of product formation and product dissociation could be revealed. To explain the substrate concentration dependency of the catalytic reaction, two types of surface sites and two products desorption pathways (a direct desorption pathway and a reactant-assisted desorption pathway) have been evoked (Fig. 2(e)). More importantly, individual nanoparticles revealed different selectivity in these two pathways. In a follow-up study by the same group, the relationship of Au nanoparticle size and the catalytic activity was carefully analyzed [29], revealing that the size of nanocatalysts strongly influences its product formation and dissociation rates coupled with surface restructuring. They also applied this strategy to explore the kinetics of electrocatalysis on individual carbon nanotubes [31] as well as single platinum (Pt) nanoparticles [32]. Majima and coworkers [22] also employed this strategy in a photocatalysis system, in which a fluorogenic probe was used to study reactive oxygen species such as singlet oxygen ($^1O_2$), and hydroxyl radicals ($\cdot$OH) generated from irradiated TiO_2 photocatalysts. Alivisatos's group studied the photocatalytic oxidation reaction of Amplex Red to resorufin using Sb-doped TiO_2 nanorods [33].

Super-resolution imaging of single particle nanocatalysis For large catalytic particles, where the size of catalytic particles is above 100 nm to even micrometer (μm), their surface structures and distributions of active sites are relatively easy to be imaged by electron microscopes, but difficult for optical microscopes owing to the existence of optical diffraction limit. To solve this problem, a fluorescent spot generated from a catalytic generated fluorescent product could be fitted by a two dimensional Gaussian function, resulting a point spread function (PSF) of single-molecule fluorescence, which allows the imaging of individual product formation event on single nanoparticles with a resolution of tens of nanometers.

A series of pioneer work on super optical resolution imaging of heterogeneous catalysis were also conducted by Chen's group. They used this method to map catalytic activity distribution and its temporal evolution on pseudo-0D, −1D, and −2D nanocatalysts [34–36]. In these studies, the catalytic formation of resorufin was used in conjunction with Gaussian fitting of PSF to achieve a sub-particle mapping of the reactive centers with a resolution of ca. 40 nm. To take mesoporus silica-coated Au nanorods as an example of pseudo-1D nanocatalysts [34] (Fig. 3(a)), the reactivity of the end sites on the nanorods was found much active center sites and their side facets, revealing a linear gradient from the middle toward the two ends along the side facets of a single Au nanorod (Fig. 3(c)). Furthermore, the reaction activity of the side cites over the center cites, differs for individual Au nanorods and depends on their length. A subsequent study on single Au nanoplates as an example of pseudo-2D nanocatalysts [35], reveals that their corner regions were most catalytic active, followed by edge regions and then flat facets (Fig. 3(d)). These site-specific activity patterns are attributed to an underlying defect density gradient that presumably formed during the seeded growth of the nanocrystals. These results indicate that identifying the active crystal planes is not enough to extrapolate the catalytic activity of metal nanoparticles. Recent investigations by the same group have led to the elucidation of the relationship between the size and catalytic activity by statistically analyzing over 1000 nanoparticles, and their results are able to screen the activity of a large amount of catalyst particles [36].

Majima and coworkers used super-resolution imaging of photocatalytic reduction to identify active sites on single TiO_2 crystals [37] and also found a crystal facet-dependent catalytic activity behavior for the reductive photocatalysis. Monitoring the catalytic turnover on micro-sized anatase crystals revealed that catalytic active sites are mainly reside at the {101} facets. They then extended the super-resolution imaging studies to Au nanoparticle-decorated TiO_2 nanoparticles [38], micrometer-sized crystals [39] and 2D nanocrystals [40]. In a very recent work, this group developed novel fluorogenic molecule probes to visualize photo-induced redox reactions on single TiO_2 and Au-TiO_2

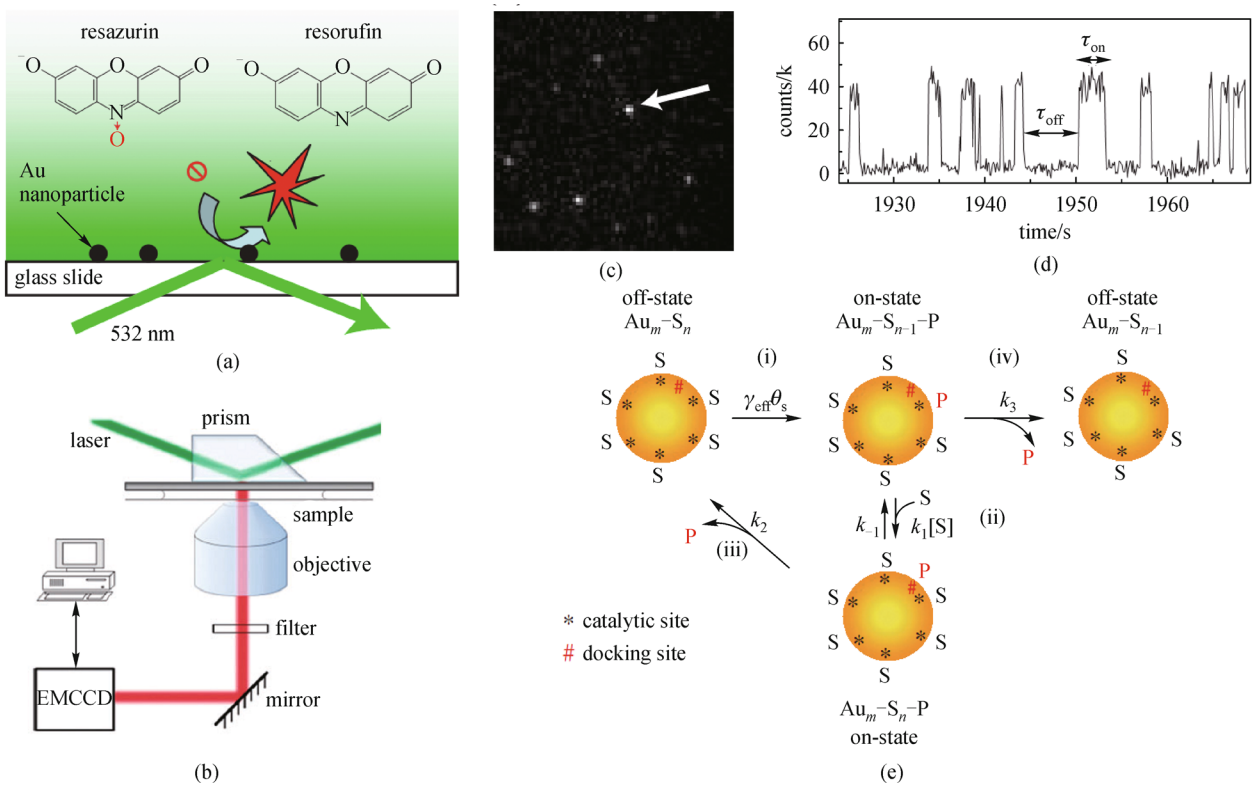

Fig. 2 Single-molecule detection of fluorogenic catalytic reactions on single Au nanoparticles. (a) Experimental design using fluorogenic catalytic reaction, surface immobilized catalysts, and total internal reflection fluorescence microscopy; (b) schematic of a prism-based TIRFM and a microfluidic reactor cell made between a slide and a coverslip; (c) a typical image (~18 μm× 18 μm) of fluorescent products on 6 nm pseudospherical Au nanoparticles during catalysis taken at 100 ms per frame; (d) a segment of the fluorescence trajectory from the fluorescence spot marked by the arrow in (c); (e) schematic diagram of the kinetic mechanism of catalysis. Au_m: Au nanoparticle; S: resazurin; P: resorufin. Au_m–S_n represents an Au nanoparticle having n adsorbed substrate molecules. The fluorescence state (on or off) of the nanoparticle is indicated at each reaction stage. Figures 2(a) to 2(d) were reproduced with permission from Ref. [23], copyright 2008 Nature Publishing Group. Figure 2(e) was reproduced with permission from Ref. [29], copyright 2010 American Chemical Society

nanoparticles [40]. By chemically modifying the fluorescent probe, the fluorescence quantum efficiency and life time were enhanced. As a result, electron transfer on the surface of the nanocatalysts can be visualized in aqueous environments with significantly improved signal-to-noise ratio. This system was used for super-resolution mapping of reactive sites with an accuracy of approximately 8 nm on Au-TiO_2 nanoparticles (Figs. 3(e) and 3(f)).

This approach was also adopted by Hofkens' group. Using the method called nanometer accuracy by stochastic chemical reactions (NASCA), Hofkens and coworkers [41] observed single catalytic turnovers on individual ZSM-22 crystals (Fig. 3(g)) and ZSM-5 crystals (Fig. 3(h)) to elucidate the influence of nanoscale features. The reconstructed fluorescence maps clearly revealed the location of the active intergrowth region. They also studied the Ti-MCM-41 catalyzed epoxidation (Fig. 3(i)) of a fluorogenic BODIPY derivative and obtained the turnover mapping on individual crystals [42]. Data analysis over an extended timeframe demonstrates that the product formation was limited to the outer regions (200–300 nm) of the individual catalyst particles.

To take a short summarize, single-molecule fluorescence microcopy allows for the real time, high-throughput observation of catalytic processes on a wide range of catalyst materials under ambient conditions with single-turnover resolution. However, TIRF does not reflect the heterogeneous in catalytic reaction due to the heterogeneities of catalyst itself. Another limitation is that single-molecule fluorescence microscopy requires either products or reactants should be fluorescent and could not be neither enhanced nor quenched by catalysts. Then, the fluorescent products must be dissociated from the catalyst surface after a short period of stay. Thus, the implication of single-molecule fluorescence microcopy in catalytic reaction is quite limited.

2.2 Surface-enhanced Raman spectroscopy

Reactants and products in catalytic reactions often exhibit fingerprint vibrational features that are related to their chemical structures, which can be measured by Raman spectroscopy. Because the Raman signals of molecules can be greatly enhanced (~10^6) in the vicinity of an excited

plasmonic material (typically Au or silver (Ag)), surface-enhanced Raman spectroscopy (SERS) [43–47] and tip-enhanced Raman spectroscopy (TERS) are capable of single molecule detection and single nanoparticle catalysis study in real time [48–51].

Kang et al. monitored the plasmon-driven dimerizing reaction of p-nitrothiophenol (pNTP) into p,p′-dimercaptoazobenzene (DMAB) on single Ag particles using SERS [52,53]. The Ag catalyst particle was relatively large (~2 μm diameter), but its surface was roughed with nanostructures, acting as an efficient SERS substrate (Fig. 4(a)). They studied the laser wavelength- and power-dependent conversion rates of the reaction on individual Ag particles and found that 532 nm excitation could accelerate the reaction rate effectively than 633 nm excitation, confirming that the reaction is induced by excitation of surface plasmon on the Ag particle. Moreover, they further found that dimerization of p-aminothiophenol (pATP) into DMAB was actually induced by the efficient energy transfer (plasmonic heating) from surface plasmon resonance to the surface adsorbed pATP, where O_2 (as an electron acceptor) is the necessary oxidant and H_2O (as a deprotonation agent) can dramatically accelerate the reaction (Fig. 4(d)) [54]. Their results demonstrated that surface plasmon assisted catalysis (SPAC) hold great promise for the studying chemical reactions on plasmonic metal nanostructures.

Combining the confocal Raman microscope with high-resolution scanning probe microscopy [e.g., atomic force microscopy (AFM) and scanning transmission microscopy (STM)], usually called TERS, allows for ultrahigh spatially resolving of spectroscopic information even with single-molecule resolution. Using the setup combining a confocal Raman microscope and an AFM, Weckhuysen and coworkers [55] used TERS to investigate a photocatalytic reaction of a self-assembled monolayer of pNTP molecules adsorbed on a gold nanoplate support. The silver-coated AFM tip acted as both the Raman signal enhancer and the catalyst (Fig. 4(e)). They monitored the photocatalytic reduction of pNTP to DMAB at the illuminated Ag tip. The reaction was initiated with a 532 nm laser, whereas a 633 nm laser was used for Raman excitation. By acquiring the Raman spectra of the molecules as a function of 532 nm illumination time (Fig. 4(f)), they found that the catalytic reaction was occurred. Moreover, the complete monolayer coverage of the pNTP reactant was disturbed during catalysis, through either the change in functionality from NO_2 to NH_2 or dimerization. In the meantime, Xu et al. [56] used a high vacuum TERS to investigate the plasmon-driven *in situ* chemical reaction of 4-nitrobenzenethiol dimerizing to dimercaptoazobenzene, which can be controlled by the plasmon intensity.

Owing to its high chemical structure sensitivity and selectivity, SERS and TERS reveal the potential to offer a general, direct, quantitative, real-time detection method for reactant consumption and product generation on a single catalyst particle, and hold tremendous promise toward the identification of atomic-scale active sites in heterogeneous catalysis. Additionally, Raman scattering is label-free and a non-invasive spectroscopic technique, thus SERS and TERS allow for the investigation of arbitrary substrates. However, these methods lack millisecond-scale temporal resolution and require the use of roughened substrate as Raman enhancer. Single-molecule sensitivity via SERS is possible in both liquid and gaseous environments, but liquid-phase catalysis experiments by TERS are difficult, because reactant/product molecules in the near surface region are hard to exclude from those specifically adsorbed to the catalyst.

3 Optical responses from catalysts

Heterogeneous catalysis reactions that involve redox always cause changes in the physical and chemical properties of the catalyst particles and the atoms in the catalyst during the catalytic cycle, which can also be measured by optical methods. Therefore, monitoring the performance of catalyst particles in real time becomes another effective approach to study nanocatalysis.

3.1 Localized surface plasmon resonance microscopy

Localized surface plasmon resonance (LSPR), is the collective coherent oscillation of conduction electrons in metal nanoparticles especially Au and Ag nanoparticles [57–59]. Owing to their unique plasmonic properties that surprisingly highly sensitive to their size, shape, composition, and charge density as well as local dielectric environment, Au and Ag nanostructures have long been utilized for nanoplasmonic chemical and biologic sensing, counting, tracking and imaging system [60–65]. In addition to high sensitivity, plasmonic nanostructures provide higher intensity, nonblinking, optical stability and easiness to prepare compared with previously reported methods.

Direct localized surface plasmon resonance monitoring of single plasmonic particle nanocatalysis Catalytic reactions can change the physical and chemical properties of a plasmonic catalyst nanoparticle because of changes of the local environment due to the consumption of reactants and generation of products on the catalyst surfaces. These changes result in the LSPR wavelength shifts in the visible/near-infrared regime. The scattering spectrum of individual nanoparticles can be monitored by dark field microscopy (DFM) [66]. These facilitate the locally probing catalytic reactions in real time by either direct or indirect strategy.

For gold nanoparticles (Au NPs), which play an important role in heterogeneous catalysis, their LSPR spectra can be measured directly to monitor the catalytic

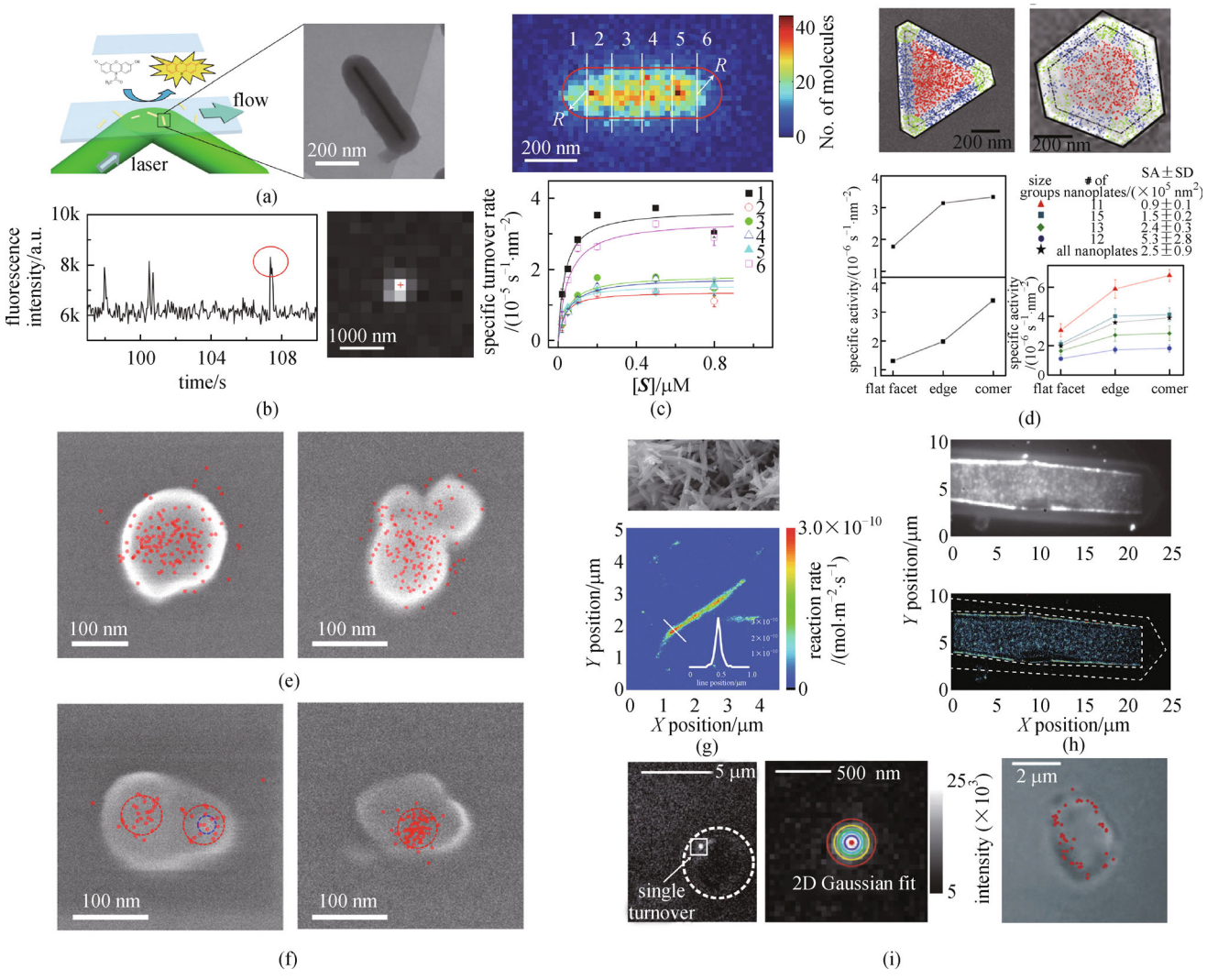

Fig. 3 Super-resolution imaging of single particle nanocatalysis. (a) Fluorogenic reaction converts a nonfluorescent molecule (Amplex Red) to a fluorescent molecule (resorufin) catalyzed by individual Au@mSiO$_2$ nanorods; (b) fluorescence intensity versus time trajectory for a single Au@mSiO$_2$ nanorod under catalysis, and wide-field fluorescence pattern during one burst (red circled); (c) subparticle distribution of reactivity map obtained for a gold nanorod. Segmentation of the nanorods clearly shows substrate concentration-dependent turnover rate in different regions; (d) spatially resolved activity quantitation on single Au@mSiO$_2$ nanoplates; (e) and (f) spatial distributions of fluorescence spots collected from TiO$_2$ (e) and 14 nm Au/TiO$_2$ particles (f); (g) super-resolution reaction map showing a single needle like ZSM-22 particle; (h) reconstructed fluorescence maps showing the location of the active intergrowth region on a ZSM-5 crystal; (i) turnover mapping on Ti-MCM-41 particles. Figures 3(a), 3(b), and 3(c) were reproduced with permission from Ref. [34], copyright 2012 Nature Publishing Group. Figure 3(d) was reproduced with permission from Ref. [35], Figs. 3(e) and 3(f) were reproduced with permission from Ref. [40], copyright 2013 American Chemical Society. Figures 3(g), 3(h), and 3(i) were reproduced with permission from Refs. [41,42], copyright 2009, 2010 Wiley

reactions occurring on their surfaces. As pioneered by Mulvaney's groups [67], the electron injection and extraction of a single Au decahedron nanoparticle were monitored during an oxidation of ascorbic acid by dissolved oxygen. The oxidation of ascorbic acid molecules caused electron injection into the Au nanoparticle, resulting in a ~20 nm blue shift of the nanoparticle's LSPR spectrum in the first 3 min. The subsequent reaction of the Au nanoparticle with O_2 depopulated the accumulated electrons, and concurrently the LSPR spectrum red-shifted back to the initial state (Figs. 5(b) and 5(c)). They calculated the electron injected rate was 4600 electrons per second. The kinetics of atomic deposition onto a single Au nanorod (Fig. 5(d)) was also studied by using this strategy. Recently, Baumberg's group upgraded DFM with supercontinuum laser source to improve its temporal resolution and real time monitored the growth of nanocrystals [68].

Yi et al. [69] used a similar strategy to quantify electron transfer rates on different facets of single gold nanoparticles during catalytic reactions. The 4-nitrophenol reduction reaction caused electron density changes on high-index facets of elongated tetrahexahedryl Au nanoparticles and

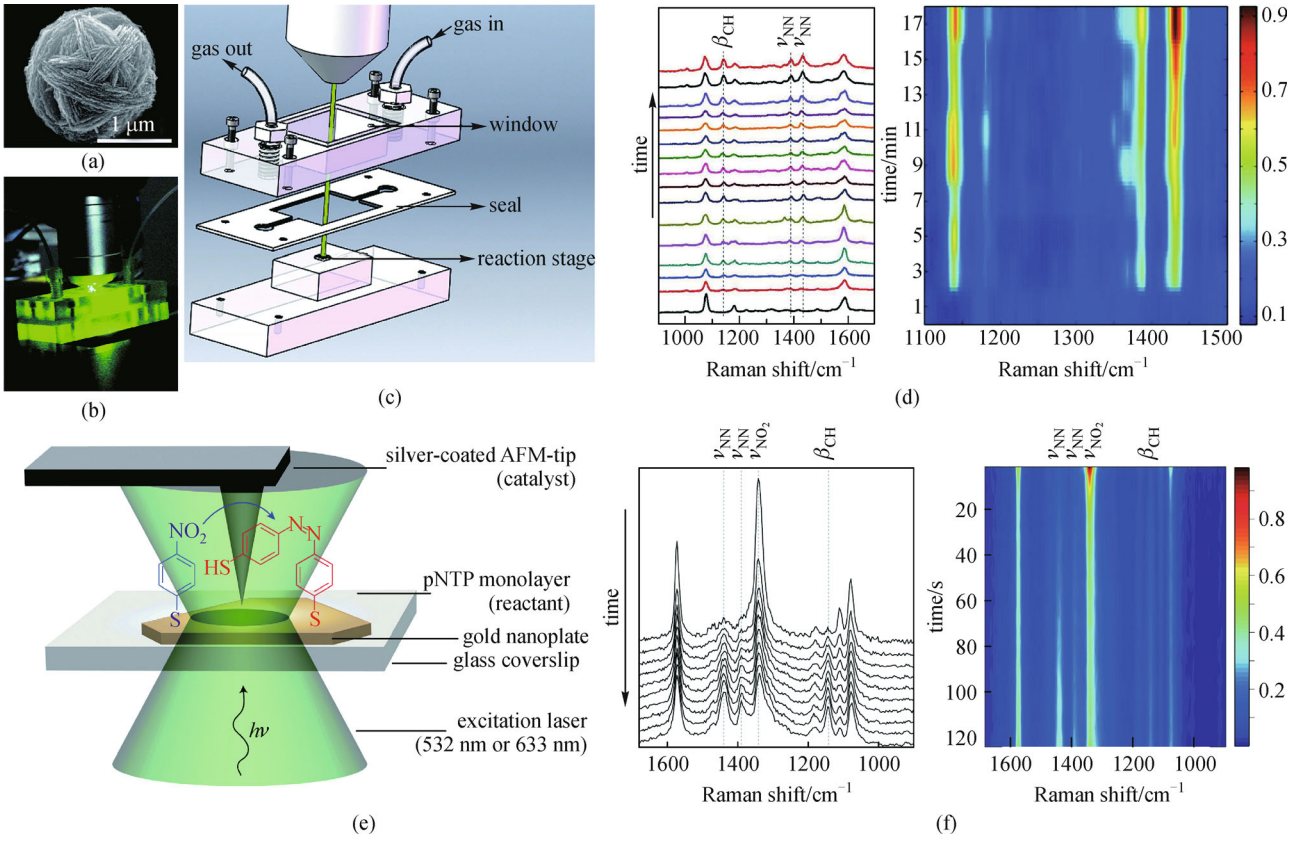

Fig. 4 Surface/tip-enhanced Raman spectroscopy for single particle nanocatalysis. (a) Scanning electron microscopy (SEM) image of a single roughened Ag microsphere with nanostructured surface; (b) photo of the gas flow cell for monitoring the surface plasmon assisted catalysis reaction under controlled gas atmosphere; (c) structure schematic of the designed reaction station; (d) time-dependent SERS spectra of 4ATP under continuous 633 nm laser excitation taken every 1 min, and series shown as a color-coded intensity map; (e) schematic overview of the experimental setup for TERS combining confocal Raman and atomic force microscope; (f) time-dependent SERS spectra acquired with the setup for TERS of the photocatalytic reduction of pNTP (top spectrum) to DMAB, and series shown as a color-coded intensity map. Figures 4(a), 4(b), and 4(c) were reproduced with permission from Ref. [54], copyright 2013 Nature Publishing Group. Figures 4(d) and 4(e) were reproduced with permission from Ref. [55], copyright 2012 Nature Publishing Group

low-index facets of Au nanorods (Figs. 5(h) and 5(i)). They observed that the high-index facets were capable of accepting electrons 7 times faster and emitting electrons 2.5 times faster than the low-index facets.

Indirect localized surface plasmon resonance monitoring of single particle nanocatalysis Unlike Au or Ag, many materials do not support a measurable LSPR signal. To solve this problem, several indirect LSPR sensing strategies have been developed. Larsson et al. [70,71] used arrays of Au nanodisks as an indirect platform to continuously monitor gas-phase reaction at the ensemble level. Recent works by Alivisatos and coworkers [72] developed an Au nanoantenna-based strategy and enable the study chemical properties at a single arbitrary nanoparticle. They used electron beam lithography to position an Au nanostructure at nanometer distances away from a palladium (Pd) nanoparticle. Pd nanoparticles could absorb hydrogen strongly and react with it to form PdH, which changes their electrical properties in a reversible manner; meanwhile, Au nanoparticles are sensitive to dielectric environment and exhibit the best plasmonic scattering features in visible region. Hydrogen gas uptake of Pd nanoparticle changed the dielectric of the single Au nanostructure, causing a shift in its LSPR spectrum (Figs. 6(a) and 6(b)). They suggested that the presence of 33 Torr hydrogen gas induced a 10 nm shift in the maximum LSPR wavelength and the sensitivity was highly dependent on the spatial distance between Pd and Au, as well as the geometry of the Au nanostructures (Fig. 6(c)). This group [73] further extended this indirect strategy to study catalysis on similar hybrid nanostructures (Au@Pd core-shell nanoparticles). They found that the shape, faceting, and Pd shell thickness of Au nanoparticles play essential role in hydrogen uptake trajectories. Using a similar strategy, Song and coworkers [74] studied the decomposition of lactic acid into hydrogen on a single chemically synthesized Au nanostructure capsulated by a platinized CdS shell. The kinetic analysis of the LSPR wavelength shift allowed for calculation of the rate constant, diffusion coefficient, as well as average distance

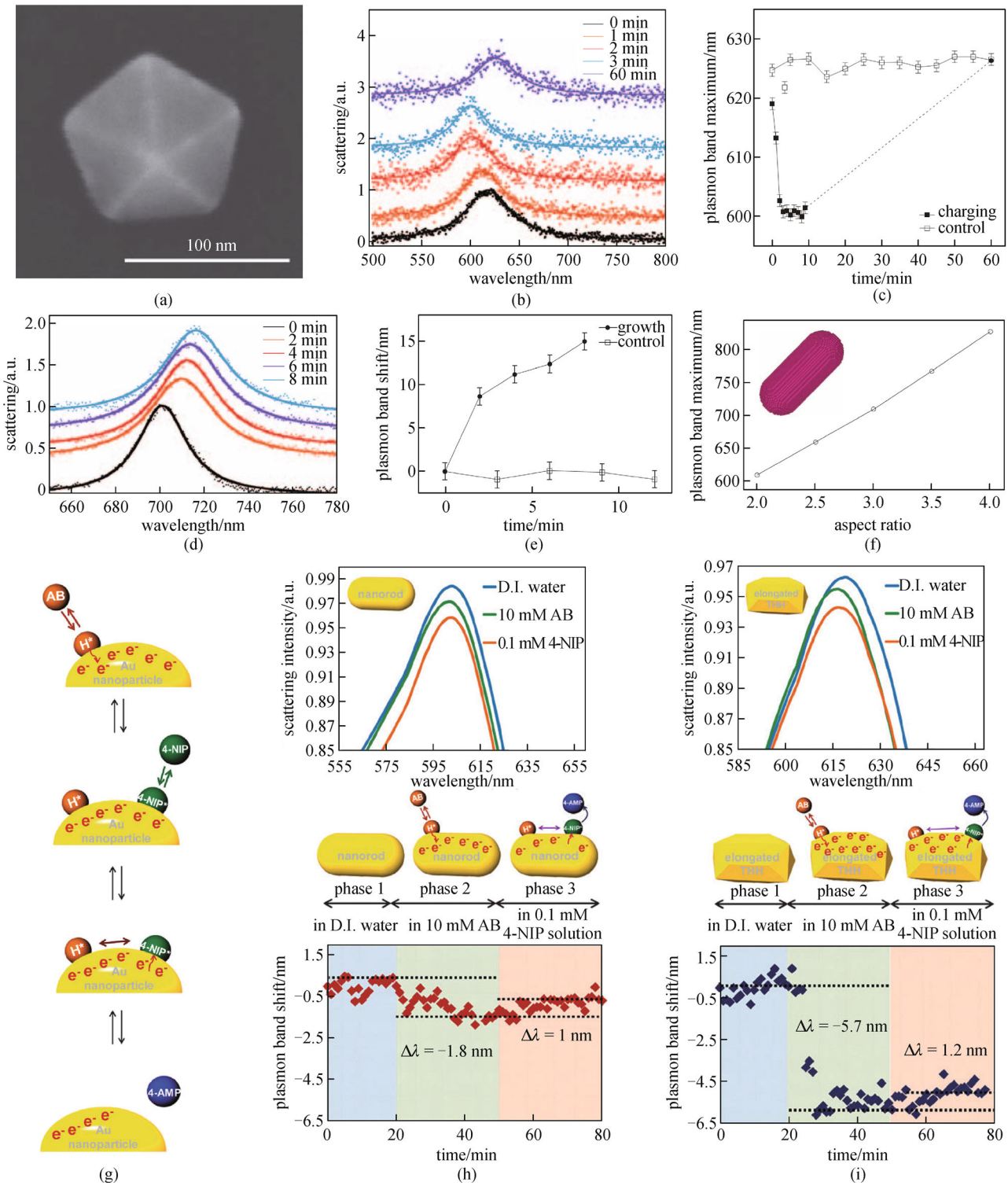

Fig. 5 Direct localized surface plasmon resonance monitoring of single plasmonic particle nanocatalysis. (a) Scanning electron microscopy (SEM) image of gold decahedron; (b) scattering spectra of nanoparticle *vs.* time after electron injection by ascorbate ions; (c) spectral shift as a function of time for the catalysis reaction and for the control experiment; (d) evolution of the scattering spectrum of a gold nanorod (aspect ratio 2.87) after a growth solution is added; (e) spectral shift as a function of time for a growth experiment and for a control experiment; (f) predicted surface plasmon position versus aspect ratio for hemispherically capped rods based on DDA results; (g) scheme for the reduction of 4-nitrophenol, catalyzed by gold nanoparticles with ammonia borane as the reducing agent. AB: ammonia borane; 4-NIP: 4-nitrophenol; 4-AMP: 4-aminophenol; (h) and (i) evolution of the scattering spectrum and surface plasmon band position of a gold nanorod (h) and an elongated tetrahexahedral gold nanoparticle (i) as a function of time after introducing water, 10 mM[1)] AB, and 0.1 mM 4-NIP, sequentially. Figures 5(a) to 5(f) were reproduced with permission from Ref. [67], copyright 2008 Nature Publishing Group. Figures 5(g), 5(h), and 5(i) were reproduced with permission from Ref. [69], copyright 2013 Royal Society of Chemistry

1) 1 mM = 1 mmol·L^{-1}

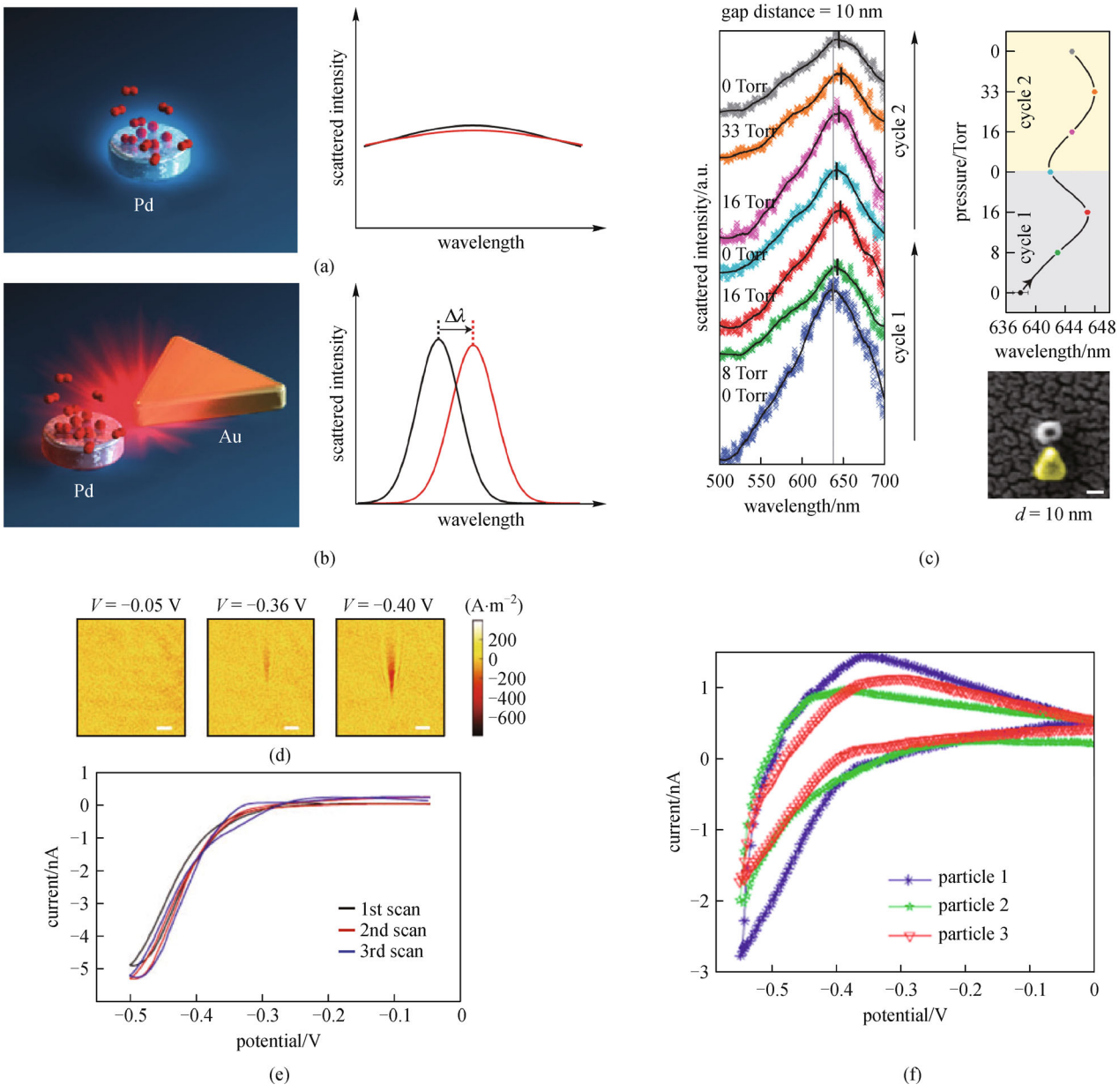

Fig. 6 Indirect localized surface plasmon resonance monitoring of single particle nanocatalysis. (a) Hydrogen adsorption on a Pd nanoparticle induces minimal wavelength shift in its scattering spectrum; (b) hydrogen sensing with a plasmonic Au nanostructure-antenna enhanced single Pd nanoparticle; (c) maximum scattering wavelength from the Au antenna depends on hydrogen partial pressure; (d) surface plasmon resonance electrochemical current density images of a single Pt nanoparticle at different potentials; (e) cyclic voltammogram of the same single nanoparticle obtained by integrating the current density over the images in (d); (f) typical cyclic voltammograms of three different single Pt nanoparticles. Figures 6(a) to 6(c) were reproduced with permission from Ref. [72], Figs. 6(d) to 6(f) were reproduced with permission from Ref. [77], copyright 2011, 2012 Nature Publishing Group

between active sites of Pt/CdS and the Au domains, and showed significant particle-to-particle heterogeneity. Liu et al. [75] investigated the dissociation and uptake of hydrogen on 15-nm Pd films on individual Au nanostructures coated with a thin SiO_2 shell as plasmonic reporters.

Tao and coworkers introduced a plasmonic film-supported nanoparticle for the study of electrocatalysis reaction with a plasmonic-based electrochemical current microscope (P-ECM). Compared with the above mentioned core@shell nanoparticles, they used a plasmonic metal film as the reporter rather than plasmonic particles. The principle of P-ECM is that the Faradaic current is determined by the generation rate of reaction products (or the consumption rate of reactants) in an electrochemical reaction process, which can be imaged by SPR because of

the sensitive dependence of SPR signal to the local concentration changes of reactants or products [76]. They first used this strategy to image local electrochemical processes and then extended it to study the electrocatalytic activity of single Pt nanoparticles and low-density arrays of nanoparticles supported on an Au film [77]. This strategy, allowing the measurement of cyclic voltammograms of multiple Pt nanoparticles individually (Figs. 6(d)–6(f)), is not only limited to electrocatalysis, but also other catalytic reactions.

This indirect plasmonic antenna mediated strategy enables LSPR to monitor other catalytic reaction using nonplasmonic nanoparticles. In addition, numerical simulations solving Maxwell equation could be used to predict changes of LSPR signals responding to physical or chemical properties changes of a particle during a catalytic reaction.

There still remain some challenges in monitoring chemical reactions with this nanoplasmonic approach, and this technique is currently not amenable to study nanocatalysis with single turnover resolution. First, Mie's light scattering theory suggests that the scattering cross-section of a particle with diameter (d) is proportional to d^6. With a conventional DFM, one can hardly measure the scattering spectrum of nanoparticles with a diameter smaller than 50 nm, which is too big to be a highly active nanocatalyst. The nanoplasmonic catalysts possesses many catalytic active sites, as a result, many reactions occur simultaneously on one catalyst particle, which make it difficult to trace single turnover. While for smaller nanoparticles, specialized instrument with more detecting sensitivity (such as electron-multiplying charge-coupled device, EMCCD) are needed to visualize. Secondly, real-time single-molecule kinetics studies are also limited by the integration time needed to acquire a spectrum (several seconds), considering that almost all of the catalytic reactions are accomplished in less than one second.

3.2 X-ray spectroscopy and microscopy

X-ray absorption spectroscopy (XAS) involves the excitation of core-level electrons of atoms, and the near-edge features and extended fine structures inform its oxidation state and local coordination environment. Therefore, XAS, including X-ray absorption near-edge structure (XANES) and extended X-ray absorption fine structure (EXAFS), has been widely used to characterize bulk solids or an ensemble of nanoparticle catalysts [78,79]. One way to measure catalysis on single nanoparticles and in situ nanoscale image of catalysts is performing X-ray absorption spectroscopy and X-ray microscopy with ~10 – 40 nm spatial resolution using synchrotron sources [80].

A powerful X-ray microscopy method is scanning transmission X-ray microscopy (STXM), which has been developed in recent years to reveal spatial heterogeneities within supported metal catalyst materials at nanoscale. Many *in situ* STXM studies of working catalysts have since appeared, mainly from the Weckhuysen's group. Individual working SiO_2-supported Fe-based Fischer-Tropsch synthesis (FTS) catalyst particles have been investigated in great detail by de Smit et al. [81] with soft X-rays (200 – 2000 eV). Constructed by analyzing the spatially resolved XAS spectra, the authors showed chemical contour maps of the catalyst (Figs. 7(a) and 7(b)), which implied intraparticle heterogeneities, as it was found that the active Fe was heterogeneously distributed within the SiO_2 binder. Furthermore, they proposed that iron carbide formed in the iron-rich region, and the presence of hydrocarbon species in iron-deficient regions suggested a spillover of products from the metal to the support, preventing the blocking of the active sites of the catalyst (Fig. 7(c)). In another STXM experiment, a microbeam X-ray absorption fine structure (μ-XAFS) spectroscopy investigation has been performed by Tada and colleagues [82]. They probed the reforming of methane to produce syngas on an industrially relevant $NiO_x/Ce_2Zr_2O_y$ catalyst material, and revealed the presence of catalytically active and inactive phases within an individual catalyst particle (Figs. 7(d)–7(f)).

Besides X-ray transmission detection modes, transmission X-ray microscopy can also be conducted with other detection modes, such as photoelectron emission and X-ray fluorescence [79]. Advances in X-ray technology have pushed the spatial resolution to 10 nm, even at high temperature and pressure [83], meanwhile, subtle designs of nanoreactor can further allow for high-throughput, 3D chemical/structural imaging in high-pressure gaseous and liquid systems [80]. But the working distance between X-ray focusing optics and the sample is short, which puts a strain on the nanoreactor design. Acquiring STXM images can require tens of minutes, which causes it difficult to track catalytic processes in real time. The long time, high intensity irradiation of X-ray can incur significant damage to the sample (both catalysts and reactants), making it unsuitable for examining a single, small, less than 10 nm catalyst particle.

4 Conclusions and outlook

In this paper, we reviewed several optical approaches that allow for the study of catalysis on single nanoparticles. Distinguished by advantages and limitations with regard to chemical selectivity, sensitivity, and spatial resolution, these approaches can give complementary and corroborating information. Nonetheless, in the field of nanoscale heterogeneous catalysis, greater highly space- and time-resolved monitoring and imaging of heterogeneities within catalytic processes are still the major challenge. New approaches remain to be developed and explored to investigate an individual catalyst particle with atomic-scale resolution and single-molecule sensitivity

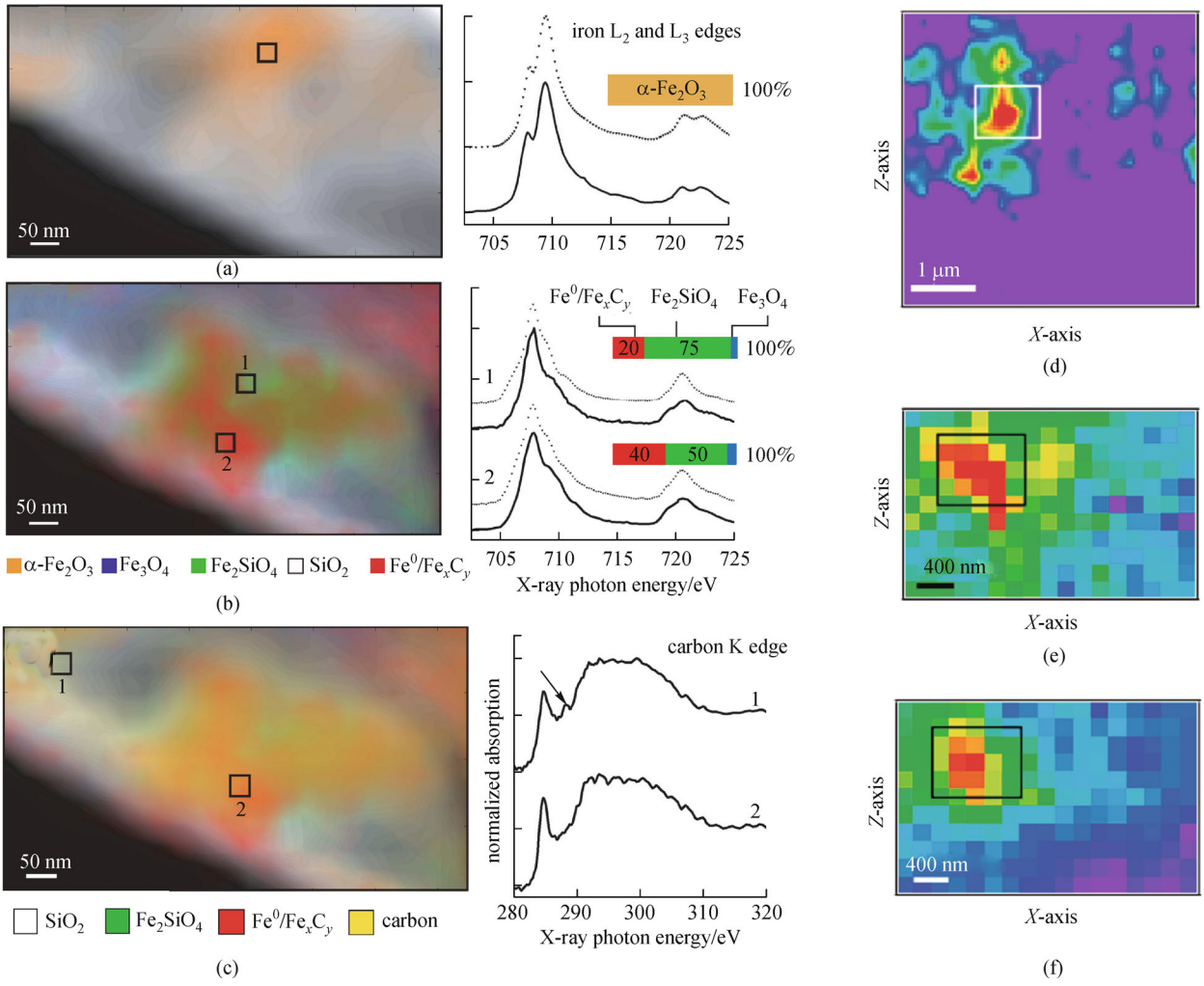

Fig. 7 Single particle nanocatalysis studies based on X-ray spectroscopy and microscopy. (a) and (b) Chemical contour maps of a 400 nm × 750 nm region and corresponding iron L_2- and L_3-edge X-ray absorption spectra of a SiO_2-supported Fe-based Fischer-Tropsch synthesis catalyst particle (a) before and (b) after 4 h in synthesis gas at 250°C; (c) scanning transmission X-ray microscopy (STXM) images of a catalyst under working conditions reveals the preferential presence of carbidic C in Fe-rich areas; (d) 2D-scanning Ni Kα (7478 eV) X-ray fluorescence (XRF) map of $NiO_x/Ce_2Zr_2O_7$ by X-ray excitation at 8428 eV; (e) Ni Kα (7478 eV) and (f) Ce Lα (4840 eV) + Lβ (5262 eV) XRF mapping images of $NiO_x/Ce_2Zr_2O_8$ by X-ray excitation at 8428 eV. Figuress 7(a), 7(b), and 7(c) were reproduced with permission from Ref. [81], copyright 2008 Nature Publishing Group. Figures 7(d), 7(e), and 7(f) were reproduced with permission from Ref. [82], copyright 2011 Royal Society of Chemistry

under true reaction conditions even high temperatures and pressures.

Some developments in other scientific fields are referable. For example, in the past 10 years we have seen the discovery of several appropriate experimental approaches, particularly developed for life sciences (e.g., stimulated emission depletion (STED) [84], fluorescence photoactivated localization microscopy (FPALM) [85] and stochastic optical reconstruction microscopy (STORM) [86]), that allow determining both axial and lateral positions of individual fluorescent molecules with nanometer accuracy. A similar trend toward increasing 2D and 3D imaging capabilities can be found in the field of X-ray microscopy. X-rays have very short wavelengths and are therefore ideally suited for achieving high spatial resolution. X-ray-based tomography and combining diffraction imaging with STXM are capable of bringing the spatial resolution down to 10 nm [87,88]. It is expected that the introduction of these advanced methods to the field of heterogeneous catalysis, will further increase our understanding of the 3D architecture and heterogeneity of complex catalytic solids as well as their reaction mechanisms.

Acknowledgements This work was supported by the National Natural Science Foundation of China (Grant Nos. 21222508) and the Shanghai Municipal Commission for Science and Technology (No. 13QH1402300).

References

1. Bell A T. The impact of nanoscience on heterogeneous catalysis. Science, 2003, 299(5613): 1688–1691
2. Weckhuysen B M. Chemical imaging of spatial heterogeneities in catalytic solids at different length and time scales. Angewandte Chemie International Edition, 2009, 48(27): 4910–4943
3. Weckhuysen B M. Preface: recent advances in the in-situ characterization of heterogeneous catalysts. Chemical Society Reviews, 2010, 39(12): 4557–4559
4. Buurmans I L C, Weckhuysen B M. Heterogeneities of individual catalyst particles in space and time as monitored by spectroscopy. Nature Chemistry, 2012, 4(11): 873–886
5. Cordes T, Blum S A. Opportunities and challenges in single-molecule and single-particle fluorescence microscopy for mechanistic studies of chemical reactions. Nature Chemistry, 2013, 5(12): 993–999
6. Wang W, Tao N. Detection, counting, and imaging of single nanoparticles. Analytical Chemistry, 2014, 86(1): 2–14
7. Gellman A J, Shukla N. Nanocatalysis: more than speed. Nature Materials, 2009, 8(2): 87–88
8. Murzin D Y. Nanokinetics for nanocatalysis. Catalysis Science & Technology, 2011, 1(3): 380–384
9. Zhang S, Nguyen L, Zhu Y, Zhan S, Tsung C K, Tao F F. In-situ studies of nanocatalysis. Accounts of Chemical Research, 2013, 46 (8): 1731–1739
10. Tao A R, Habas S, Yang P D. Shape control of colloidal metal nanocrystals. Small, 2008, 4(3): 310–325
11. Xia Y, Xiong Y, Lim B, Skrabalak S E. Shape-controlled synthesis of metal nanocrystals: simple chemistry meets complex physics? Angewandte Chemie International Edition, 2009, 48(1): 60–103
12. Langille M R, Personick M L, Zhang J, Mirkin C A. Defining rules for the shape evolution of gold nanoparticles. Journal of the American Chemical Society, 2012, 134(35): 14542–14554
13. Cox J T, Zhang B. Nanoelectrodes: recent advances and new directions. Annual Review of Analytical Chemistry, 2012, 5(1): 253–272
14. Ebejer N, Güell A G, Lai S C S, McKelvey K, Snowden M E, Unwin P R. Scanning electrochemical cell microscopy: a versatile technique for nanoscale electrochemistry and functional imaging. Annual Review of Analytical Chemistry, 2013, 6(1): 329–351
15. Lu H P, Xun L, Xie X S. Single-molecule enzymatic dynamics. Science, 1998, 282(5395): 1877–1882
16. Edman L, Foldes-Papp Z, Wennmalm S, Rigler R. The fluctuating enzyme: a single molecule approach. Chemical Physics, 1999, 247 (1): 11–22
17. Paige M F, Fromm D P, Moerner W E. Biomolecular applications of single-molecule measurements: kinetics and dynamics of a single enzyme reaction. Proceedings-Society of Photo-Optical Instrumentation Engineers, 2002, 4634: 92–103
18. Velonia K, Flomenbom O, Loos D, Masuo S, Cotlet M, Engelborghs Y, Hofkens J, Rowan A E, Klafter J, Nolte R J M, de Schryver F C. Single-enzyme kinetics of CALB-catalyzed hydrolysis. Angewandte Chemie International Edition, 2005, 44(4): 560–564
19. English B P, Min W, van Oijen A M, Lee K T, Luo G, Sun H, Cherayil B J, Kou S C, Xie X S. Ever-fluctuating single enzyme molecules: Michaelis-Menten equation revisited. Nature Chemical Biology, 2006, 2(2): 87–94
20. Smiley R D, Hammes G G. Single molecule studies of enzyme mechanisms. Chemical Reviews, 2006, 106(8): 3080–3094
21. Roeffaers M B J, Sels B F, Uji-I H, de Schryver F C, Jacobs P A, de Vos D E, Hofkens J. Spatially resolved observation of crystal-face-dependent catalysis by single turnover counting. Nature, 2006, 439 (7076): 572–575
22. Naito K, Tachikawa T, Fujitsuka M, Majima T. Real-time single-molecule imaging of the spatial and temporal distribution of reactive oxygen species with fluorescent probes: Applications to TiO_2 photocatalysts. Journal of Physical Chemistry C, 2008, 112(4): 1048–1059
23. Xu W, Kong J S, Yeh Y T E, Chen P. Single-molecule nanocatalysis reveals heterogeneous reaction pathways and catalytic dynamics. Nature Materials, 2008, 7(12): 992–996
24. Janssen K P F, de Cremer G, Neely R K, Kubarev A V, Van Loon J, Martens J A, de Vos D E, Roeffaers M B J, Hofkens J. Single molecule methods for the study of catalysis: from enzymes to heterogeneous catalysts. Chemical Society Reviews, 2014, 43(4): 990–1006
25. Chen P, Zhou X, Andoy N M, Han K S, Choudhary E, Zou N, Chen G, Shen H. Spatiotemporal catalytic dynamics within single nanocatalysts revealed by single-molecule microscopy. Chemical Society Reviews, 2014, 43(4): 1107–1117
26. Tachikawa T, Majima T. Single-molecule, single-particle approaches for exploring the structure and kinetics of nanocatalysts. Langmuir, 2012, 28(24): 8933–8943
27. Chen P, Xu W L, Zhou X C, Panda D, Kalininskiy A. Single-nanoparticle catalysis at single-turnover resolution. Chemical Physics Letters, 2009, 470(4–6): 151–157
28. Xu W, Kong J S, Chen P. Probing the catalytic activity and heterogeneity of Au-nanoparticles at the single-molecule level. Physical Chemistry Chemical Physics, 2009, 11(15): 2767–2778
29. Zhou X, Xu W, Liu G, Panda D, Chen P. Size-dependent catalytic activity and dynamics of gold nanoparticles at the single-molecule level. Journal of the American Chemical Society, 2010, 132(1): 138–146
30. Chen P, Zhou X, Shen H, Andoy N M, Choudhary E, Han K S, Liu G, Meng W. Single-molecule fluorescence imaging of nanocatalytic processes. Chemical Society Reviews, 2010, 39(12): 4560–4570
31. Xu W, Shen H, Kim Y J, Zhou X, Liu G, Park J, Chen P. Single-molecule electrocatalysis by single-walled carbon nanotubes. Nano Letters, 2009, 9(12): 3968–3973
32. Han K S, Liu G, Zhou X, Medina R E, Chen P. How does a single Pt nanocatalyst behave in two different reactions? A single-molecule study. Nano Letters, 2012, 12(3): 1253–1259
33. Xu W, Jain P K, Beberwyck B J, Alivisatos A P. Probing redox photocatalysis of trapped electrons and holes on single Sb-doped titania nanorod surfaces. Journal of the American Chemical Society, 2012, 134(9): 3946–3949
34. Zhou X, Andoy N M, Liu G, Choudhary E, Han K S, Shen H, Chen P. Quantitative super-resolution imaging uncovers reactivity patterns on single nanocatalysts. Nature Nanotechnology, 2012, 7 (4): 237–241

35. Andoy N M, Zhou X, Choudhary E, Shen H, Liu G, Chen P. Single-molecule catalysis mapping quantifies site-specific activity and uncovers radial activity gradient on single 2D nanocrystals. Journal of the American Chemical Society, 2013, 135(5): 1845–1852
36. Zhou X C, Choudhary E, Andoy N M, Zou N M, Chen P. Scalable parallel screening of catalyst activity at the single-particle level and subdiffraction resolution. Acs Catalysis, 2013, 3(7): 1448–1453
37. Tachikawa T, Yamashita S, Majima T. Evidence for crystal-face-dependent TiO_2 photocatalysis from single-molecule imaging and kinetic analysis. Journal of the American Chemical Society, 2011, 133(18): 7197–7204
38. Bian Z F, Tachikawa T, Kim W, Choi W, Majima T. Superior electron transport and photocatalytic abilities of metal-nanoparticle-loaded TiO_2 superstructures. Journal of Physical Chemistry C, 2012, 116(48): 25444–25453
39. Wang N, Tachikawa T, Majima T. Single-molecule, single-particle observation of size-dependent photocatalytic activity in Au/TiO_2 nanocomposites. Chemical Science, 2011, 2(5): 891–900
40. Tachikawa T, Yonezawa T, Majima T. Super-resolution mapping of reactive sites on titania-based nanoparticles with water-soluble fluorogenic probes. ACS Nano, 2013, 7(1): 263–275
41. Roeffaers M B J, de Cremer G, Libeert J, Ameloot R, Dedecker P, Bons A J, Bückins M, Martens J A, Sels B F, de Vos D E, Hofkens J. Super-resolution reactivity mapping of nanostructured catalyst particles. Angewandte Chemie International Edition, 2009, 48(49): 9285–9289
42. de Cremer G, Roeffaers M B J, Bartholomeeusen E, Lin K, Dedecker P, Pescarmona P P, Jacobs P A, de Vos D E, Hofkens J, Sels B F. High-resolution single-turnover mapping reveals intra-particle diffusion limitation in Ti-MCM-41-catalyzed epoxidation. Angewandte Chemie International Edition, 2010, 49(5): 908–911
43. Nie S, Emory S R. Probing single molecules and single nanoparticles by surface-enhanced Raman scattering. Science, 1997, 275(5303): 1102–1106
44. Kneipp K, Wang Y, Kneipp H, Perelman L T, Itzkan I, Dasari R, Feld M S. Single molecule detection using surface-enhanced Raman scattering (SERS). Physical Review Letters, 1997, 78(9): 1667–1670
45. Brus L. Noble metal nanocrystals: plasmon electron transfer photochemistry and single-molecule Raman spectroscopy. Accounts of Chemical Research, 2008, 41(12): 1742–1749
46. Stiles P L, Dieringer J A, Shah N C, Van Duyne R P. Surface-enhanced Raman spectroscopy. Annual Review of Analytical Chemistry, 2008, 1(1): 601–626
47. Sonntag M D, Klingsporn J M, Zrimsek A B, Sharma B, Ruvuna L K, Van Duyne R P. Molecular plasmonics for nanoscale spectroscopy. Chemical Society Reviews, 2014, 43(4): 1230–1247
48. Bailo E, Deckert V. Tip-enhanced Raman scattering. Chemical Society Reviews, 2008, 37(5): 921–930
49. Pettinger B. Single-molecule surface- and tip-enhanced Raman spectroscopy. Molecular Physics, 2010, 108(16): 2039–2059
50. Kim H, Kosuda K M, Van Duyne R P, Stair P C. Resonance Raman and surface- and tip-enhanced Raman spectroscopy methods to study solid catalysts and heterogeneous catalytic reactions. Chemical Society Reviews, 2010, 39(12): 4820–4844
51. Sonntag M D, Klingsporn J M, Garibay L K, Roberts J M, Dieringer J A, Seideman T, Scheidt K A, Jensen L, Schatz G C, Van Duyne R P. Single-molecule tip-enhanced Raman spectroscopy. Journal of Physical Chemistry C, 2012, 116(1): 478–483
52. Kang L, Xu P, Zhang B, Tsai H, Han X, Wang H L. Laser wavelength- and power-dependent plasmon-driven chemical reactions monitored using single particle surface enhanced Raman spectroscopy. Chemical Communications, 2013, 49(33): 3389–3391
53. Kang L L, Xu P, Chen D T, Zhang B, Du Y C, Han X J, Li Q, Wang H L. Amino acid-assisted synthesis of hierarchical silver microspheres for single particle surface-enhanced Raman spectroscopy. Journal of Physical Chemistry C, 2013, 117(19): 10007–10012
54. Xu P, Kang L, Mack N H, Schanze K S, Han X, Wang H L. Mechanistic understanding of surface plasmon assisted catalysis on a single particle: cyclic redox of 4-aminothiophenol. Scientific Reports, 2013, 3: 2997
55. van Schrojenstein Lantman E M, Deckert-Gaudig T, Mank A J G, Deckert V, Weckhuysen B M. Catalytic processes monitored at the nanoscale with tip-enhanced Raman spectroscopy. Nature Nanotechnology, 2012, 7(9): 583–586
56. Sun M, Zhang Z, Zheng H, Xu H. In-situ plasmon-driven chemical reactions revealed by high vacuum tip-enhanced Raman spectroscopy. Scientific Reports, 2012, 2: 647
57. Willets K A, Van Duyne R P. Localized surface plasmon resonance spectroscopy and sensing. Annual Review of Physical Chemistry, 2007, 58(1): 267–297
58. Henry A I, Bingham J M, Ringe E, Marks L D, Schatz G C, Van Duyne R P. Correlated structure and optical property studies of plasmonic nanoparticles. Journal of Physical Chemistry C, 2011, 115(19): 9291–9305
59. Ringe E, Sharma B, Henry A I, Marks L D, Van Duyne R P. Single nanoparticle plasmonics. Physical Chemistry Chemical Physics, 2013, 15(12): 4110–4129
60. Anker J N, Hall W P, Lyandres O, Shah N C, Zhao J, Van Duyne R P. Biosensing with plasmonic nanosensors. Nature Materials, 2008, 7(6): 442–453
61. Stewart M E, Anderton C R, Thompson L B, Maria J, Gray S K, Rogers J A, Nuzzo R G. Nanostructured plasmonic sensors. Chemical Reviews, 2008, 108(2): 494–521
62. Zheng X, Liu Q, Jing C, Li Y, Li D, Luo W, Wen Y, He Y, Huang Q, Long Y T, Fan C. Catalytic gold nanoparticles for nanoplasmonic detection of DNA hybridization. Angewandte Chemie International Edition, 2011, 50(50): 11994–11998
63. Liu Q, Jing C, Zheng X, Gu Z, Li D, Li D W, Huang Q, Long Y T, Fan C. Nanoplasmonic detection of adenosine triphosphate by aptamer regulated self-catalytic growth of single gold nanoparticles. Chemical Communications, 2012, 48(77): 9574–9576
64. Shi L, Jing C, Ma W, Li D W, Halls J E, Marken F, Long Y T. Plasmon resonance scattering spectroscopy at the single-nanoparticle level: real-time monitoring of a click reaction. Angewandte Chemie International Edition, 2013, 52(23): 6011–6014
65. Li K, Qin W, Li F, Zhao X, Jiang B, Wang K, Deng S, Fan C, Li D. Nanoplasmonic imaging of latent fingerprints and identification of cocaine. Angewandte Chemie International Edition, 2013, 52(44): 11542–11545
66. Langhammer C, Larsson E M. Nanoplasmonic in situ spectroscopy for catalysis applications. Acs Catalysis, 2012, 2(9): 2036–2045

67. Novo C, Funston A M, Mulvaney P. Direct observation of chemical reactions on single gold nanocrystals using surface plasmon spectroscopy. Nature Nanotechnology, 2008, 3(10): 598–602
68. Herrmann L O, Baumberg J J. Watching single nanoparticles grow in real time through supercontinuum spectroscopy. Small, 2013, 9 (22): 3743–3747
69. Eo M, Baek J, Song H D, Lee S, Yi J. Quantification of electron transfer rates of different facets on single gold nanoparticles during catalytic reactions. Chemical Communications, 2013, 49(45): 5204–5206
70. Larsson E M, Langhammer C, Zorić I, Kasemo B. Nanoplasmonic probes of catalytic reactions. Science, 2009, 326(5956): 1091–1094
71. Langhammer C, Larsson E M, Kasemo B, Zorić I. Indirect nanoplasmonic sensing: ultrasensitive experimental platform for nanomaterials science and optical nanocalorimetry. Nano Letters, 2010, 10(9): 3529–3538
72. Liu N, Tang M L, Hentschel M, Giessen H, Alivisatos A P. Nanoantenna-enhanced gas sensing in a single tailored nanofocus. Nature Materials, 2011, 10(8): 631–636
73. Tang M L, Liu N, Dionne J A, Alivisatos A P. Observations of shape-dependent hydrogen uptake trajectories from single nanocrystals. Journal of the American Chemical Society, 2011, 133(34): 13220–13223
74. Seo D, Park G, Song H. Plasmonic monitoring of catalytic hydrogen generation by a single nanoparticle probe. Journal of the American Chemical Society, 2012, 134(2): 1221–1227
75. Tittl A, Yin X, Giessen H, Tian X D, Tian Z Q, Kremers C, Chigrin D N, Liu N. Plasmonic smart dust for probing local chemical reactions. Nano Letters, 2013, 13(4): 1816–1821
76. Shan X, Patel U, Wang S, Iglesias R, Tao N. Imaging local electrochemical current via surface plasmon resonance. Science, 2010, 327(5971): 1363–1366
77. Shan X, Díez-Pérez I, Wang L, Wiktor P, Gu Y, Zhang L, Wang W, Lu J, Wang S, Gong Q, Li J, Tao N. Imaging the electrocatalytic activity of single nanoparticles. Nature Nanotechnology, 2012, 7 (10): 668–672
78. Frenkel A I, Rodriguez J A, Chen J G G. Synchrotron techniques for in situ catalytic studies: capabilities, challenges, and opportunities. Acs Catalysis, 2012, 2(11): 2269–2280
79. Bordiga S, Groppo E, Agostini G, van Bokhoven J A, Lamberti C. Reactivity of surface species in heterogeneous catalysts probed by in situ X-ray absorption techniques. Chemical Reviews, 2013, 113(3): 1736–1850
80. Beale A M, Jacques S D M, Weckhuysen B M. Chemical imaging of catalytic solids with synchrotron radiation. Chemical Society Reviews, 2010, 39(12): 4656–4672
81. de Smit E, Swart I, Creemer J F, Hoveling G H, Gilles M K, Tyliszczak T, Kooyman P J, Zandbergen H W, Morin C, Weckhuysen B M, de Groot F M F. Nanoscale chemical imaging of a working catalyst by scanning transmission X-ray microscopy. Nature, 2008, 456(7219): 222–225
82. Tada M, Ishiguro N, Uruga T, Tanida H, Terada Y, Nagamatsu S, Iwasawa Y, Ohkoshi S. μ-XAFS of a single particle of a practical $NiO_x/Ce_2Zr_2O_y$ catalyst. Physical Chemistry Chemical Physics, 2011, 13(33): 14910–14913
83. Chao W, Fischer P, Tyliszczak T, Rekawa S, Anderson E, Naulleau P. Real space soft X-ray imaging at 10 nm spatial resolution. Optics Express, 2012, 20(9): 9777–9783
84. Hell S W. Toward fluorescence nanoscopy. Nature Biotechnology, 2003, 21(11): 1347–1355
85. Hess S T, Girirajan T P K, Mason M D. Ultra-high resolution imaging by fluorescence photoactivation localization microscopy. Biophysical Journal, 2006, 91(11): 4258–4272
86. Huang B, Wang W, Bates M, Zhuang X. Three-dimensional super-resolution imaging by stochastic optical reconstruction microscopy. Science, 2008, 319(5864): 810–813
87. Chao W, Harteneck B D, Liddle J A, Anderson E H, Attwood D T. Soft X-ray microscopy at a spatial resolution better than 15 nm. Nature, 2005, 435(7046): 1210–1213
88. Thibault P, Dierolf M, Menzel A, Bunk O, David C, Pfeiffer F. High-resolution scanning X-ray diffraction microscopy. Science, 2008, 321(5887): 379–382

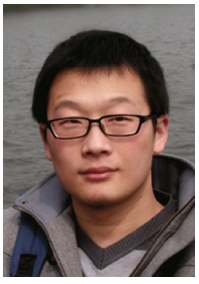

Kun Li received his B.S. degree in Applied Chemistry from Shandong University of Science and Technology in 2009. Currently he is a Ph.D. candidate in the Division of Physical Biology at Shanghai Institute of Applied Physics (SINAP), Chinese Academy of Sciences (CAS), under the supervisor of Prof. Chunhai Fan and Prof. Di Li. His research interests are the assembly of nanoplasmonic particles for biosensing and bioimaging.

Weiwei Qin received her B.S. degree in Chemistry from Ludong University in 2011. Currently, she is a Ph.D. candidate at Shanghai Institute of Applied Physics (SINAP), Chinese Academy of Sciences (CAS). Her research focuses on the use of nanoplasmonic antenna in the study of single-molecule enzymology.

Yan Xu received her B.S. degree in Biological Engineering from Henan University of Science and Technology in 2010, and the M. S. degree in Microbiology from Nanjing Agricultural University in 2013. Now she is a Ph.D. student in the Division of Physical Biology at Shanghai Institute of Applied Physics (SINAP), Chinese Academy of Sciences (CAS). Her research focuses on the single-molecule fluorescence, super-resolution imaging to understand DNAzyme catalysis.

Tianhuan Peng received his B.S. degree in Applied Chemistry from Beijing University of Chemical Technology in 2012. Currently he is a Ph.D. student in the Division of Physical Biology at Shanghai Institute of Applied Physics (SINAP), Chinese Academy of Sciences (CAS). His research focuses on the surface-enhanced Raman scattering (SERS) mapping in bioimaging.

Di Li is a Professor of the Division of Physical Biology at Shanghai Institute of Applied Physics (SINAP), Chinese Academy of Sciences (CAS). He received his B.S. degree (2000) in Environmental Engineering from Dalian University of Technology and Ph.D. degree (2005) in Chemistry from Changchun Institute of Applied Chemistry, Chinese Academy of Sciences. After post-doctoral research with Prof. Itamar Willner at the Hebrew University of Jerusalem, he joined SINAP in 2008. He won “National Natural Science Fund for Excellent Young Scholar” in 2012. He has published over 60 papers with over 3600 times citations. His current research focuses on using single nanoplasmonic particle in bioimaging and nanocatalysis.